21

Spatial modulation of terahertz radiation using optical vortex generators based on thin films of single-walled carbon nanotubes

© E.G. Tsyplakova , A.V. Radivon[1], M.I. Paukov[1], G.M. Katyba[2], N.I. Raginov[3], A.V. Chernykh[4], A.S. Ezerskii[4], I.I. Rakov[1], A.V. Arsenin[1], I.E. Spektor[5], K.I. Zaitsev[5], D.V. Krasnikov[3], N.V. Petrov[4,6], A.G. Nasibulin[3], V. Volkov[1], M.G. Burdanova[1,2]

[1] Center for Photonics and Two-Dimensional Materials, Moscow Institute of Physics and Technology (National Research University), Dolgoprudny, Russia
[2] Osipyan Institute of Solid State Physics RAS, Chernogolovka, Russia
[3] Skolkovo Institute of Science and Technology, Moscow, Russia
[4] ITMO University, St. Petersburg, Russia
[5] Prokhorov Institute of General Physics, Russian Academy of Sciences, Moscow, Russia
[6] Harbin Engineering University Innovation and Development Center, Qingdao, China

E-mail: burdanova.mg@mipt.ru

Received February 05, 2025
Revised February 20, 2025
Accepted February 28, 2025

The results of a study of the performance of an orbital angular momentum modulator in the submillimeter range (340 GHz) based on thin films of single-walled carbon nanotubes are presented. Spiral zone wafers have been created to characterize the spatial modulation of the Gaussian beam using a state-of-the-art technique for synthesizing and depositing nanostructures of different thicknesses on the substrate. Using a combination of spiral zone plates allows the energy in the terahertz beam to be redistributed across the different generated optical vortices. The fabricated diffractive elements have tunable characteristics such as redistributable orbitally angular momentum and charge number. The obtained orbital angular momentum generators can be integrated into next-generation communication systems.

Keywords: carbon nanotubes, spatial modulation of terahertz radiation, tunable optical element, spiral zone plate, optical vortex.

DOI: 10.61011/EOS.2025.03.61165.15-25

Introduction

Due to active advancements in terahertz (THz) radiation sources and detectors, their application scope has expanded — including biomedical applications [1], microscopy [2], spectroscopy, security, and high-speed data transmission [3]. Nevertheless, the development of these technologies has been stymied by the inadequacy of the current base of optical elements required for signal processing [4]. Solving this problem requires finding suitable materials, device geometries with the ability to accurately control operating parameters.

Particularly for diverse applications including magnetic property determination, Bose-Einstein condensate monitoring, wireless communications, plasmon-polariton generation, and terahertz imaging, the development of terahertz-band optical vortex generators has become essential [5]. Their usefulness in these applications is attributable to the fact that vortices are characterized by orbital angular momentum, and the possibility of decomposing the beam into vortex modes can increase the information capacity of optical channels in information transmission [6]. The development of orbital angular momentum modulators, however, has received little attention to date. Among the approaches available for this purpose are varifocal rotational metasurface systems, but this method requires a complex procedure for creating metasurfaces, and this solution is also poorly capable of creating tunable optical elements [7].

Adaptive optical elements operating in the THz range require materials with high and tunable conductivity in the THz range, as well as mechanical and chemical stability [8,9]. One such material is thin films of single-walled carbon nanotubes (SWCNT). In addition to the above properties, SWNT films can be scalably reproducible and deposited on any substrate by dry transfer [10,11]. Taken together, these advantages make it possible to actively use SWNT to create elements of THz optics — sources [{]12, detectors [13], lenses [14], modulators [8], tunable diffraction gratings [15], and others. Nevertheless, the use of SWCNT films as generators of THz optical vortices has not yet been realized, although the structures based on them can be tuned by various parameters — stretching [16], electrochemical doping [9], pulsed optical pumping power [17], and the presence of gas medium [18].

This work presents, for the first time, a terahertz (THz) optical vortex generator based on thin films of single-walled carbon nanotubes (SWCNTs), designed as a spiral zone plate (SZP). The spirals considered here are thin, i.e. the width of the line at the center is comparable to the width of the line at a radius distance from the center. Compared

to previously presented vortex modulators, the described device demonstrates a simple approach to improve vortex beam modulation (orbital angular momentum control). Moreover, its fabrication has been improved with ultra-thin, compact CNT-based devices. SZP is created thanks to advanced nanotube film production technologies and a reliable method of depositing them with the required geometry on the substrate. The paper shows the multifunctionality of SZP as well as its behavior depending on the thickness of SWNT films.

Methods

Pattern creation based on single-walled carbon nanotubes

The SWNTs used to create the spiral zone plates were synthesized by aerosol chemical vapor deposition (CVD) [19]. An elastomer (Silpuran, Wacker) with a thickness of $t = 0$, 1 mm, transparent in the terahertz range, was used as a substrate to deposit the SWNT pattern. The primary stage of patterning on the substrate is the creation of a metal mask by pulsed laser ablation to produce slits in the form of spirals with thickness of $150-200\,\mu$m (Fig. 1). An IPG fiber laser operating in the frequency range of $1060-1070$ nm (pulse duration $\tau = 100$ ns, pulse repetition rate $\nu = 20$ kHz, pulse energy $E = 1$ mJ) was used for the laser ablation process. The laser beam was moved on the mask surface was by a galvano-optical mirror system using a focusing F-Theta lens with focal length of $F = 207$ nm to ensure uniform irradiation of the surface. The pattern was then applied to a nitrocellulose hydrophilic filter (HAWP, Merck Millipore, pore size $0.45\,\mu$m) by pulling the filter with an attached metal mask through rollers to compress the pores at specific locations and reduce their permeability. At the same time, the engraved mask regions did not touch the nitrocellulose filter. This allowed the deposition of SWCNT aerosol as thin films on uncompressed pore regions, replicating the mask geometry. The obtained structure was transferred by dry transfer method to the substrate (Fig. 1) [20]. The fabricated samples were characterized by high resolution of the applied pattern, its sharp edges and almost complete absence of nanotubes in the spaces between the pattern parts. In previous work, we have shown that SWCNTs synthesized by aerosole CVD have a distinctively high specific conductivity in the terahertz range ($250\,\Omega^{-1}\text{cm}^{-1}$ at frequency 1 THz). In addition, it has been shown that the conductivity increases with the increase of wavelength due to the large number of free charge carriers.

Scanning the terahertz beam behind the pattern plane

A prefabricated terahertz imaging setup was used for experimental validation of the fabricated SZP patterns (Fig. 2, a detailed description of the setup can be found, for example, in Ref. [14]). A backward-wave tube (BWT)

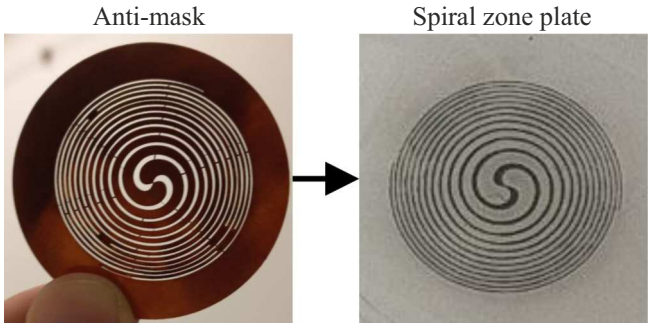

Figure 1. The procedure for fabrication of SWCNT-based SZPs. The left figure shows a copper stencil etched using pulsed laser ablation. The right figure shows a thin film of SWNTs deposited on a nitrocellulose filter with an imprinted pattern.

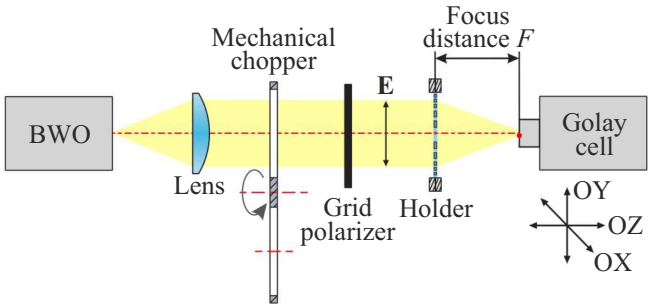

Figure 2. Schematic diagram of the experimental setup: Backward-wave tube (BWT), collimating lens, mechanical chopper, mesh polarizer, holder, Golay cell. The BWT was used as the source of THz radiation and the Golay cell was used as the detector.

was used as a source of continuous terahertz radiation. BWT operating frequency, $\nu = 340$ GHz, relative spectral width $\delta\nu/\nu \sim 10^{-5}$, output power $P = 10^{-2}$ mW, sensitivity $S_V = 10^{-5}$ V/W. After passing through the collimating lens, the beam hit the grid polarizer, acquiring linear polarization. A Golay cell with $\tau = 10^{-1}$ s response time was used as the radiation detector, and a chopper with $\nu_{mod} = 22$ Hz modulation frequency was used to modulate the radiation. A tip made of ABS type plastic with carbon impurities was fabricated to determine the intensity of the radiation. A hole with a diameter of $b = 600\,\mu$m was made inside the tip. The signal-to-noise ratio was reduced by using a combination of a collimating aspherical wide-aperture high-density polyethylene (HDPE) [21] lens and a flat-convex poly-4-methylpentene (TPX) lens focusing the terahertz radiation on the input window of the Golay cell. The back focal length of the aspheric lens is $f' = 6.62$ mm, that of the focusing lens is $f'' = 25.00$ mm, and the diameter of both lenses is $d = 25.40$ mm. The detector was mounted on a motorized slider having a positioning accuracy of $\leq 2\,\mu$m, enabling two-dimensional pixel-by-pixel scanning of the terahertz beam intensity over an area of $6 \times 6\,\text{mm}^2$ with a scanning step of $250\,\mu$m. The

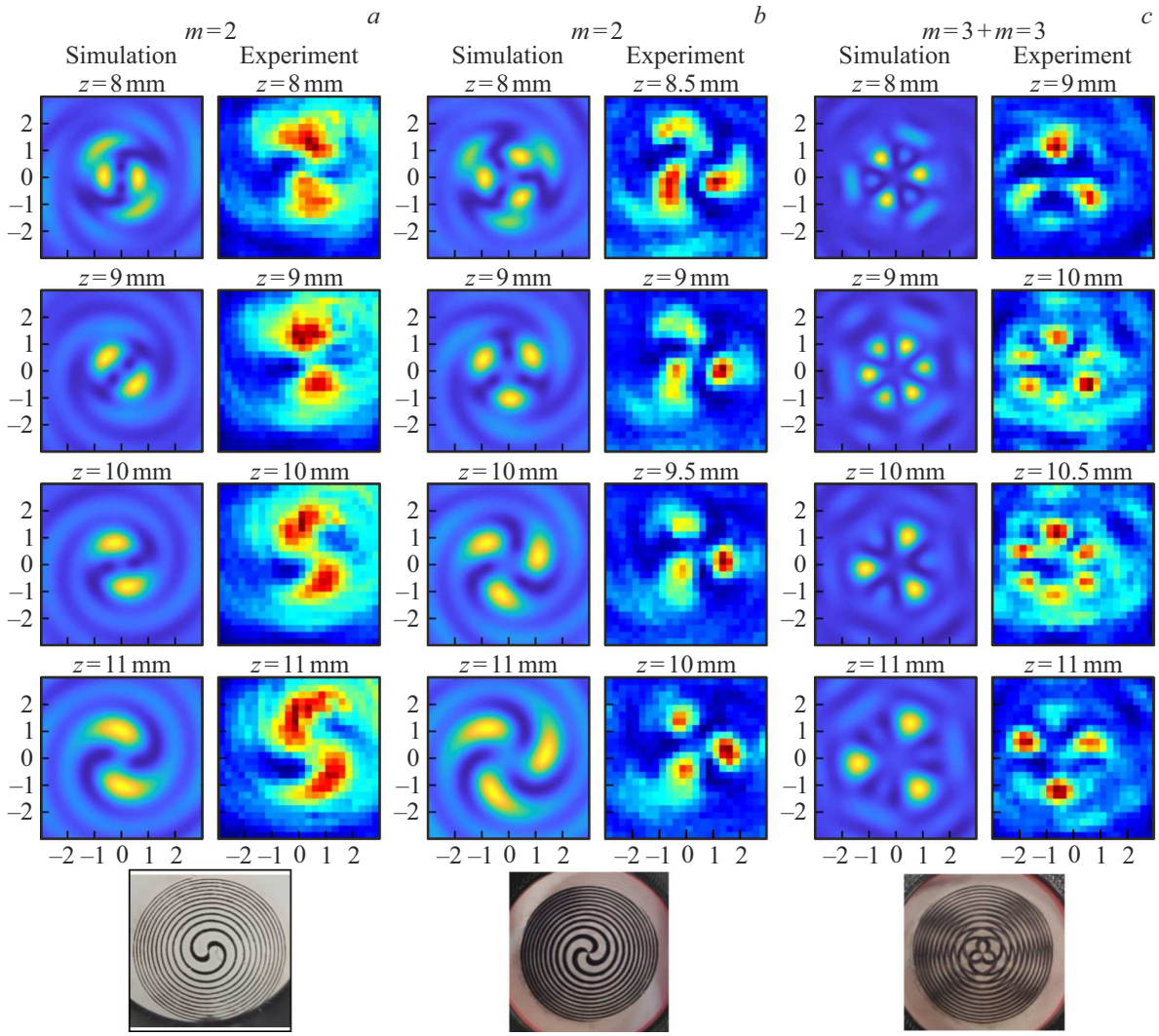

Figure 3. Transformation of THz beam passing through *a* — a double-charged SZP, *b* — a triple-charged SZP, *c* — a combination of two triple-charged SZPs. The left side of each panel shows the modeling results, the right side shows the experimental results. Pictures of the obtained elements are provided at the bottom.

spiral zone plates were mounted on a metal ring measuring $D = 50.10$ mm in diameter, which was much larger than the THz beam's diameter.

Results

Study of the parameters of single spiral zone plates

According to our concept, THz ultrathin spiral zone plates with different topological charges and focal lengths were used as individual elements for multifunctional spiral modulators (MSM). An improvised continuous THz wave imaging system was used for the experimental characterization of the fabricated THz vortex beams (Fig. 2). The spirals were located in the plane $X0Y$ (point (0,0,0) corresponds to the center of the optical vortex), and two-dimensional cross sections of the THz field intensity $I(x, y, z = \text{const})$ were recorded in the vicinity of the SZP focal spot, the distance from the optical element z was adjusted using a micrometer. The resulting $2D$-distributions of intensity are shown in Fig. 3. In particular, modelled and experimental intensity images were obtained for SZP with topological charges $m = 2$ and $m = 3$ and theoretical focal length $F = 10$ mm (Fig. 3, *a* and *b*, respectively), as well as the combination of two SZPs with topological charges $m = 3$ (Fig. 3, *c*). Two spots can be observed for the two-charge spiral and three spots can be observed for the three-charge spiral, respectively.

Study of the parameters of the rotational combination of multiple SZPs

The tunability of the MSM was demonstrated by using modulators consisting of two single identical SZPs attached close to each other with the possibility of rotation (Fig. 3, *c*).

The intensity profiles $I(x, y, z = \text{const})$ across the terahertz beam propagation direction were recorded for different distances from the bilayer SZP like in case of a single SZP. The left panel of Fig. 3, *c* shows the simulation results. The experimental focal length values agree well with the theoretical calculations to the accuracy of the scanning step along the coordinate z (0.5 mm). It should also be considered that when the spirals were combined and placed in contact, the small distance between them of 0.3 mm, representing the thickness of the substrate of each sample, introduced some ambiguity in determining the focus position.

Results and discussion

The experimental results confirm the validity of the constructed concept, but the SZP showed relatively low diffraction efficiency. This effect is most likely attributable to an imperfection of the SZP fabrication procedure occurring at the roller press stage and resulting in a slight ellipticity of the sample. The problems described can be resolved with the improved manufacturing accuracy. Also, both thickening of the samples themselves to increase absorption and broadening of the spirals in the center, reducing the zero-order influence, can improve the focusing of the described elements.

Generally, the SZP-based modulator is capable of generating different states of orbital angular momentum depending on the topological charges of the installed plates, redistributing the intensity between the target vortex and vortex-free components of these modes, and adjusting the phase shift between these modes.

The profiles of the vortex beams are essentially similar to the high order asymmetric modes in multimodal THz waveguides [22,23]. This fact makes it possible to control the excitation of high-order modes to tune multimode channels for THz wired telecommunication applications [24]. The proposed approach is wide-scalable in case of usage of the rotation of multiple SZPs for multiplexing/demultiplexing and multiplication of vortex generation.

Moreover, further development of the SZP design includes controlled adjustment of SWCNT conductivity in the THz range through optical, thermal, electrochemical, or mechanical means, influencing the SZP's functional performance.

Conclusions

A multifunctional modulator of orbital angular momentum of THz radiation based on the rotational combination of SZPs was developed in the result of this study. The designed modulator can predictably redistribute the intensity between the vortex and vortex-free components of these modes and adjust the phase shift between the modes based on the topological charges of the created plates. The efficiency of a single SZP and various combinations of multifunctional SZPs was experimentally measured, which confirmed the proposed concept of controlling the orbital angular momentum of the THz beam. The spatial rotation provides a degree of freedom for implementation of different THz modulations. The resulting beams may find promising applications in new THz imaging systems and next-generation communication systems.

Conflict of interest

The authors declare that they have no conflict of interest.

References

[1] O.A. Smolyanskaya, N.V. Chernomyrdin, A.A. Konovko, K.I. Zaytsev, I.A. Ozheredov, O.P. Cherkasova, M.M. Nazarov, J.-P. Guillet, S.A. Kozlov, Yu.V. Kistenev, J.-L. Coutaz, P. Mounaix, V.L. Vaks, J.-H. Son, H. Cheon, V.P. Wallace, Yu. Feldman, I. Popov, A.N. Yaroslavsky, A.P. Shkurinov, V.V. Tuchin. Progress in Quantum Electronics, 62, 1 (2018). DOI: 10.1016/j.pquantelec.2018.10.001

[2] R. Kersting, H.-T. Chen, N. Karpowicz, G.C. Cho. Journal of Optics A Pure and Applied Optics, **7** (2), 184 (2005). DOI: 10.1088/1464-4258/7/2/024

[3] A. Shafie, N. Yang, C. Han, J.M. Jornet, M. Juntti, T. Kürner. IEEE Network, **37** (3), 162 (2023). DOI: 10.1109/MNET.118.2200057

[4] M. Laikin. Lens Design. Optical Science and Engineering, 4th edition. (CRC Press, Boca Raton, FL, 2006).

[5] N.V. Petrov, B. Sokolenko, M.S. Kulya, A. Gorodetsky, A.V. Chernykh. Light: Advanced Manufacturing, **3** (1), 640 (2022). DOI: 10.37188/lam. 2022.043

[6] A.E. Willner, K. Pang, H. Song, K. Zou, H. Zhou. Applied Physics Reviews, **8** (4), 041312 (2021). DOI: 10.1063/5.0054885

[7] H. Moser, C. Rockstuhl. Laser and Photonics Reviews, **6**, 219 (2012). DOI: 10.1002/lpor.201000019

[8] M.G. Burdanova, G.M. Katyba, R. Kashtiban, G.A. Komandin, E. Butler-Caddle, M. Staniforth, A.A. Mkrtchyan, D.V. Krasnikov, Yu.G. Gladush, J. Sloan, A.G. Nasibulin, J. Lloyd-Hughes. Carbon, **173**, 245 (2021). DOI: 10.1016/j.carbon.2020.11.008

[9] D.S. Kopylova, D. Satko, E.M. Khabushev, A.V. Bubis, D.V. Krasnikov, T.M. Kallio, A.G. Nasibulin. Carbon, **167**, 244 (2020). DOI: 10.1016/j.carbon.2020.05.103

[10] D.A. Ilatovskii, E.P. Gilshtein, O.E. Glukhova, A.G. Nasibulin. Advanced Science, **9** (24), 2201673 (2022). DOI: 10.1002/advs.202201673

[11] D.V. Krasnikov, B.Y. Zabelich, V.Y. Iakovlev, A.P. Tsapenko, S.A. Romanov, A.A. Alekseeva, A.K. Grebenko, A.G. Nasibulin. Chemical Engineering Journal, **372**, 462 (2019). DOI: 10.1016/j.cej.2019.04.173

[12] R.R. Hartmann, J. Kono, M.E. Portnoi. Nanotechnology, **25**, 322001 (2014). DOI: 10.1088/0957-4484/25/32/32200

[13] M. Jin, Y. Wang, M. Chai, C. Chen, Z. Zhao, T. He. Advanced Functional Materials, **32** (11), 2107499 (2021). DOI: 10.1002/adfm.202107499

[14] G.M. Katyba, N.I. Raginov, E.M. Khabushev, V.A. Zhelnov, A. Gorodetsky, D.A. Ghazaryan, M.S. Mironov, D.V. Krasnikov, Yu.G. Gladush, J. Lloyd-Hughes, A.G. Nasibulin, A.V. Arsenin, V. Volkov, K.I. Zaytsev, M.G. Burdanova. Optica, **10**, 53 (2023).
DOI: 10.1364/optica.475385
[15] I.V. Novikov, N.I. Raginov, D.V. Krasnikov, S.S. Zhukov, K.V. Zhivetev, A.V. Terentiev, D.A. Ilatovskii, A. Elakshar, E.M. Khabushev, A.K. Grebenko, S.A. Kuznetsov, S.D. Shandakov, B.P. Gorshunov, A.G. Nasibulin. Chemical Engineering Journal, **485**, 149733 (2024).
DOI: 10.1016/j.cej.2024.149733
[16] M.I. Paukov, V.V. Starchenko, D.V. Krasnikov, G.A. Komandin, Yu.G. Gladush, S.S. Zhukov, B.P. Gorshunov, A.G. Nasibulin, A.V. Arsenin, V. Volkov. Ultrafast Science, **3**, 0021 (2023). DOI: 10.34133/ultrafastscience.0021
[17] M.G. Burdanova, A.P. Tsapenko, D.A. Satco, R. Kashtiban, C.D.W. Mosley, M. Monti, M. Staniforth, J. Sloan, Yu.G. Gladush, A.G. Nasibulin, J. Lloyd-Hughes. ACS Photonics, **6** (4), 1058 (2019).
DOI: 10.1021/acsphotonics.9b00138
[18] B. Arash, Q. Wang. Scientific Reports, **3**, 1782 (2013).
DOI: 10.1038/srep01782
[19] E.M. Khabushev, D.V. Krasnikov, O.T. Zaremba, A.P. Tsapenko, A.E. Goldt. The Journal of Physical Chemistry Letters, **10**, 6962 (2019). DOI: 10.1021/acs. jpclett.9b02777
[20] A. Kaskela, A.G. Nasibulin, M.Y. Timmermans, B. Aitchinson, A. Papadimitratos, Y. Tian, Z. Zhu, H. Jiang, D.P. Brown, A. Zakhidov, E.I. Kauppinen. Nano Letters, **10**, 4349 (2010).
DOI: 10.1021/nl101680s
[21] N.V. Chernomyrdin, A.O. Schadko, S.P. Lebedev, V.L. Tolstoguzov, V.N. Kurlov, I.V. Reshetov, I.E. Spektor, M. Skorobogatiy, S.O. Yurchenko, K.I. Zaitsev. Applied Physics Letters, **110**, DOI: 10.1063/1.4984952
[22] G.M. Katyba, K.V. Zaytsev, N.V. Chernomyrdin, I.A. Shikunova, G.A. Komandin, V.B. Anzin, S.P. Lebedev, I.E. Spektor, V.E. Karasik, S.O. Yurchenko, I.V. Reshetov, V.N. Kurlov, M. Skorobogatiy. Advanced Optical Materials, **6**, 1800573 (2018). DOI: 10.1002/adom.201800573
[23] K.I. Zaytsev, G.M. Katyba, N.V. Chernomyrdin, I.N. Dolganova, A.S. Kucheryavenko, A.N. Rossolenko, V.V. Tuchin, V.N. Kurlov, M. Skorobogatiy. Advanced Optical Materials, **8**, 2000307 (2020). DOI: 10.1002/adom.202000307
[24] X. Guofu, M. Skorobogatiy. Journal of Infrared, Millimeter, and Terahertz Waves, **43**, 728 (2022). DOI: 10.1007/s10762-022-00879-x

Translated by A.Akhtyamov